INTERNATIONAL JOURNAL FOR NUMERICAL METHODS IN FLUIDS
Int. J. Numer. Meth. Fluids 2003; **42**:1073–1086 (DOI: 10.1002/fld.577)

Steady/unsteady aerodynamic analysis of wings at subsonic, sonic and supersonic Mach numbers using a 3D panel method

Jeonghyun Cho, Cheolheui Han, Leesang Cho and Jinsoo Cho*,†

School of Mechanical Engineering, Hanyang University, Seoul 133-791, Republic of Korea

SUMMARY

This paper treats the kernel function of an integral equation that relates a known or prescribed upwash distribution to an unknown lift distribution for a finite wing. The pressure kernel functions of the singular integral equation are summarized for all speed range in the Laplace transform domain. The sonic kernel function has been reduced to a form, which can be conveniently evaluated as a finite limit from both the subsonic and supersonic sides when the Mach number tends to one. Several examples are solved including rectangular wings, swept wings, a supersonic transport wing and a harmonically oscillating wing. Present results are given with other numerical data, showing continuous results through the unit Mach number. Computed results are in good agreement with other numerical results. Copyright © 2003 John Wiley & Sons, Ltd.

KEY WORDS: frequency-domain panel method; kernel function; Prandtl–Glauert factor; Ackeret factor; sonic; continuity

1. INTRODUCTION

An important problem for aeroelastic analysis is to evaluate the pressure distribution of a wing in unsteady motion. The classic solution approach to the unsteady compressible flow problem has been through the use of lifting surface theory. The improvements in computational hardware capabilities in recent years makes it no longer the method of choice, even for preliminary design, the lifting surface theory still has its wide applications for the unsteady aerodynamic analysis of wings and propellers.

The kernel function technique has been used widely. Küssner [1, 2] derived the governing integral equation from the doublet of the acceleration potential for calculating the unsteady pressure distribution on a thin finite wing. The kernel function formulation relates a known or prescribed downwash distribution to an unknown load distribution for a finite wing in unsteady motion. The method has the advantage that it deals with the pressure differential and induced

*Correspondence to: Jinsoo Cho, School of Mechanical Engineering, Hanyang University, 133-179 Seoul, Korea.
†E-mail: jscho@hanyang.ac.kr

Contract/grant sponsor: Basic Research Program of the Korean Science and Engineering Foundation; contract/grant number: 1999-1-305-001-5

Received June 2001
Revised 20 March 2003

velocity of interest directly. Landahl [3, 4] derived a compact form for the formulation of the kernel function for general configurations in unsteady subsonic flow. Harder and Rodden [5] also formulated kernel functions for non-planar surfaces in supersonic flow. These pressure kernel functions led to advent of the doublet point method (DPM) [6–9], that unified subsonic [6] and supersonic flows [7]. The subsonic and supersonic DPMs can be combined into one code since they differ only in the kernel function [9]. The DPM is an extension of the doublet lattice method (DLM) [10, 11]. The DPM is much simpler than the DLM. Furthermore, the method is exact in the sense that no approximation is made to the procedure of obtaining the Laplace transform. According to Eversmann and Pitt [12], their numerical test results showed that the DPM results show a severe discrepancy for unequal spacing strips because a pivotal calculation in the method is valid only if the strip widths are constant. Eversmann and Pitt [12] suggested the use of a hybrid scheme in which the best features of the doublet lattice method and the doublet point method are combined.

The present method is based on a compressible unsteady panel method for predicting generalized force transfer functions for non-planar lifting surfaces developed by Cho and Williams [13, 14]. They applied this method to wings with various shapes and obtained good results. Their scheme resembles the 'doublet point method' of Ueda and Dowell [6, 7]. However, since the point approximation is applied only to non-singular quantities, no special care need be exercised near singularities. Any steady panel code could easily be modified to include unsteady effects, simply by multiplying the influence coefficients by appropriate phase factors.

Although the lifting surface theory should be continuous through all Mach numbers, few studies have been made in the sonic range. Beyond that the unsteady airloads are of importance to aeroelasticians in the transonic flow speed. In the two-dimensional case, the effects of compressibility may be obtained from results of incompressible theory with correction factors applied such as the well-known Prandtl–Glauert factor in subsonic flow. The Prandtl–Glauert or Ackeret rules for variation of pressure coefficient with freestream Mach number in the subsonic and supersonic flow are clearly invalid for Mach numbers near one.

Recently, Ueda [15] clarify the finite continuity of the non-coplanar kernel functions for steady flow at sonic Mach number. In the early 1950s, Runyan and Woolston [16] developed an integral method for determining the unsteady loads on a finite wing in subsonic flow including the limiting case of sonic flow.

The purpose of the present study is to define the kernel function of the singular integral equation developed by Cho and Williams [13, 14] for all speed ranges and to clarify the finite continuity of steady and unsteady flow when the Mach number equals to one. The new method is verified by showing that it produces results that are in good agreement with both steady results of Ueda [15] and unsteady ones of Runyan and Woolston [16]. The continuity of unsteady flow at sonic Mach number was not verified by Ueda [15].

2. FREQUENCY-DOMAIN PANEL METHOD

2.1. Formulation

Consider an initial value problem for linearized compressible flow in which the initial disturbances vanish away from the lifting surfaces. For the load P at a point on a lifting surface $\mathbf{x}_0$ with unit normal $\mathbf{n}_0$, a transformed pressure differential $\Delta p = \rho_\infty U_\infty P$ is assigned acting in

the direction $+\mathbf{n}_0$ (We will assume that $\mathbf{n}_0$ has no component in the freestream or x direction. The flow has speed U_∞, density ρ_∞ and Mach number M). The lifting surface induces a transformed velocity at an arbitrary point $\mathbf{x}$, in an arbitrary direction $\mathbf{n}$, which is given by an integral over the lifting surface.

$$w(\mathbf{x}) = \iint K(\mathbf{x}, \mathbf{x}_0) P(\mathbf{x}_0)\, \mathrm{d}S \tag{1}$$

The kernel is the fundamental solution of the reduced wave equation corresponding to the velocity w induced at $\mathbf{x}$ by a point load applied at $\mathbf{x}_0$. In the standard problem, w is specified on the surface and we solve for the load P. The integral is discretized, for simplicity, by a piecewise constant approximation.

$$[w] = [C][P] \tag{2}$$

where C is the integral of K over each panel, and P is to be thought of as a vector of loads on all panels. The problem then is to develop efficient methods for evaluating the coefficients C, with accuracy consistent with the discretization errors in Equation (2).

The unsteady non-planar kernel K can be abbreviated as (see Figure 1, Table I and Reference [17])

$$K = \bar{K}_p K_0 + D\mathbf{n}_0 \cdot \xi K_{p0} \tag{3}$$

where $\xi = (y - y_0)\mathbf{j} + (z - z_0)\mathbf{k}$. The quantities K_{p0} and K_0 are the steady planar and non-planar kernels, respectively. These functions are singular in the axis $\xi = 0$, $X = (x - x_0) > 0$.

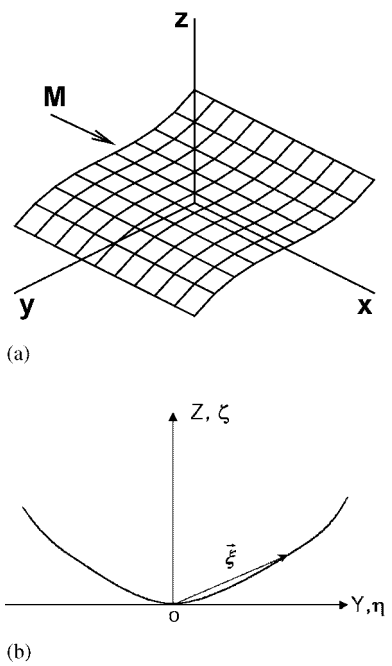

Figure 1. Non-planar lifting surface: (a) surface and panel geometry, (b) coordinate system.

Table I. Non-planar kernel functions.

Kernel functions	K_p
$M<1$	$\dfrac{e^{-\bar{s}X}}{8\pi}\left[\dfrac{Me^{\bar{s}\zeta_-}}{RR_-}+\displaystyle\int_{-\infty}^{\zeta_-}\dfrac{e^{\bar{s}v}}{(v^2+\xi^2)^{3/2}}\,dv\right]$
$M>1$	$\dfrac{e^{-\bar{s}X}}{8\pi}\left[\dfrac{Me^{\bar{s}\zeta_-}}{RR_-}+\dfrac{Me^{\bar{s}\zeta_+}}{RR_+}+\displaystyle\int_{\zeta_+}^{\zeta}\dfrac{e^{\bar{s}v}}{(v^2+\xi^2)^{3/2}}\,dv\right]$

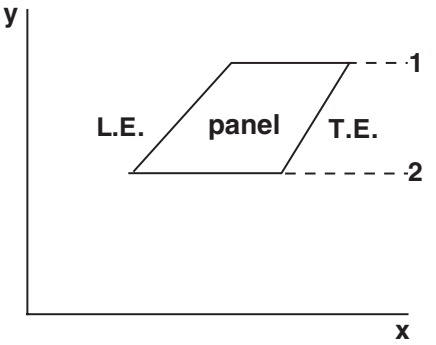

Figure 2. Quadrilateral panel.

In supersonic flow, there will be no disturbance to the flow ahead of the rearward facing Mach lines which originate at the leading most point of the lifting surface. Beyond that, the kernel functions are singular on the Mach cone emitted from the doublet point [13].

The factor $\bar{K}_p$ is the ratio of the unsteady to steady planar kernels. The coefficient D is given in terms of derivatives of $\bar{K}_p$

$$D=\mathbf{n}\cdot\left(\mathbf{i}\frac{\partial}{\partial X}+\boldsymbol{\xi}\frac{1}{\xi}\frac{\partial}{\partial\xi}\right)\bar{K}_p \tag{4}$$

where $X=x-x_0$. Note that in steady flow, $\bar{K}_p=1$ and $D=0$. The important point is that $\bar{K}_p$ is a regular function and can therefore be treated as nearly constant over the quadrilateral panel (illustrated in Figure 2), while its derivatives can be evaluated by finite differences. Therefore, the influence coefficient C is approximated by

$$C=\bar{K}_pC_0+DC_{p0} \tag{5}$$

where C_0 and C_{p0} are the steady non-planar and planar influence coefficients, respectively, which can be evaluated analytically. The unsteady factor $\bar{K}_p$ and D are evaluated at only one point on the panel.

$\bar{K}_p$ depends only on relative axial and radial separations X and ξ (which are relative distance between a field point and a panel point), as well as the Mach number and the scaled complex

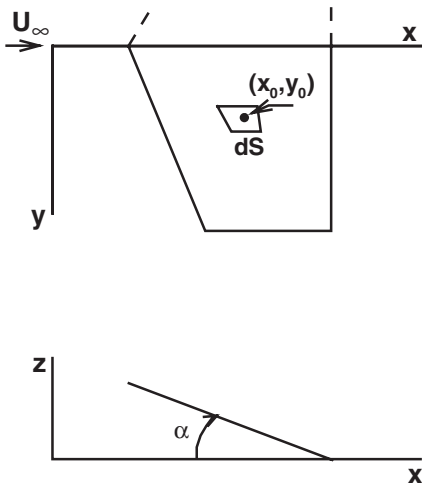

Figure 3. Wing co-ordinate system.

Laplace variables $\bar{s} = s/U$ [17, 18]. Since the function is non-dimensional, it must depend only on the products $\bar{s}X$ and $\bar{s}\xi$ [17]. In the current work we take it to be

$$\bar{K}_p = \bar{K}_p(sx, sy; M, \Phi) \tag{6}$$

where $sx = |\bar{s}|X$ and $sy = |\bar{s}|\xi$, and Φ is the argument of $\bar{s}$. The range of sx and sy are set by the largest desired magnitude of $\bar{s}$ and the geometry of the body. This range is determined *a priori*, and the function $\bar{K}_p$ is then tabulated on a rectangular grid covering the range, with a grid density which is somewhat finer than the resolution of the panelling that is to be used. Values of $\bar{K}_p$ and its derivatives are then found by interpolation in the table when the influence coefficient matrix is computed. The advantage of this scheme is that the number of kernel evaluations scales with the number of panels, rather than with the square of the number of panels as would be the case if the evaluations were done as needed. Furthermore, the table does not need to be reconstructed for any values of $\bar{s}$ with smaller magnitude than that used to define the table. This table is reconstructed only when M, Φ or the geometry is modified.

2.2. *Kernel function*

In this section, the kernel function introduced in Equation (3) is defined. Let λ be 0 if $M < 1$ and 1 if $M > 1$. For a planar wing lying in x–y plane (see Figure 3), the steady planar kernel is

$$K_{p0} = \frac{\Lambda}{4\pi R} \tag{7}$$

where

$$R^2 = X^2 + \beta Y^2$$

$$\beta = 1 - M^2$$

$$\Lambda = \frac{(1+\lambda)X + (1-\lambda)R}{Y^2}$$

When $M > 1$ and $X < 0$ it is better to use the equivalent expression, $\Lambda = \beta/(R - X)$, which is regular at $\xi = 0$.

The steady non-planar kernel can be expressed simply as

$$K_0 = \mathbf{n} \cdot \nabla(\mathbf{n}_0 \cdot \boldsymbol{\xi} K_{p0}) \tag{8}$$

The supersonic kernel is defined as 0 for any point outside the downstream Mach cone from the load point. The unsteady factor $\bar{K}_p$ is

$$\bar{K}_p = \frac{E[M(E_- + \lambda E_+) + RB]}{\Lambda} \tag{9}$$

where

$$B = \int_{\zeta_+}^{\zeta_-} \exp(\bar{s}v)/(v^2 + \xi^2)^{3/2} dv, \quad (1 - M^2)v = X - M\sqrt{X^2 + \beta\xi^2}$$

$$E = \exp(-\bar{s}X)$$

$$E_\pm = \exp(\bar{s}\zeta_\pm)/R_\pm$$

$$R_\pm = \mathrm{sqrt}[\xi^2 + (\zeta_\pm)^2]$$

$$\zeta_- = (X - MR)/\beta$$

$$\zeta_+ = \begin{cases} (X + MR)/\beta & \text{if } M > 1 \\ -\infty & \text{if } M < 1 \end{cases}$$

Although $\bar{K}_p$ is non-singular, it does need special treatment along certain lines of removable singularity. Specifically, $\bar{K}_p = E$ on $\xi = 0, X > 0$. Furthermore, in supersonic flow, the definition outside the downstream Mach cone is somewhat arbitrary. To maintain some continuity for panels which straddle the Mach cone, we take $\bar{K}_p = \exp(\bar{s}XM/\beta^2)$ at all points outside the Mach cone (this being the value on the cone at the same X). This eliminates sensitivity to whether the evaluation point on the panel happens to fall just within, or just without, the zone of dependence of the control point.

Note that $\bar{K}_p$ is continuous everywhere in the complex s-plane when $M > 1$. To define B, and therefore the solution, in $\mathrm{Re}(s) < 0$ for subsonic flow, we make use of a simple analytic continuation. Let $B(a_1, a_2)$ denote the integral with lower and upper limits a_1 and a_2. Clearly, then

$$B(-\infty, \zeta_-) = B(-\infty, -b) + B(-b, \zeta_-) = B_0 + B_1 \tag{10}$$

where b is any positive real number, and B_0 and B_1 are the infinite and finite parts, respectively. The second term, B_1 is analytic but the first term, B_0 is not defined in $\mathrm{Re}(s)<0$. Since B_0 has real support, it is sufficient to consider its continuation for $\mathrm{Im}(s)>0$. The integrand has a branch cut along $-\xi<\mathrm{Im}(v)<\xi$ on the imaginary v axis, and vanishes exponentially in the left-half v plane. Therefore, as long as $b>0$, the integration path can be turned from $(-\infty,-b)$ to $(-b,+\mathrm{i}\infty)$. The result is

$$B_0 = \int_0^\infty \mathrm{e}^{-\chi}\,\mathrm{d}r \tag{11}$$

where

$$\chi = (b-\mathrm{i}r)\bar{s} + \frac{3}{2}\ln A + \mathrm{i}\,\frac{(\pi-3\theta)}{2}$$

$$A = [(b^2+\xi^2-r^2)^2 + (2br)^2]^{1/2}$$

$$\theta = \cos^{-1}[(b^2+\xi^2-r^2)/A]$$

$$r = \sqrt{x^2+\beta(y^2+z^2)}$$

Note that B_0 is a function only of radius ξ, and so can be computed and stored once over the range of possible radii. Values for specific panel and control point combinations are obtained by interpolation. The constant b is chosen to be approximately $\xi_{\max}$, the largest radius of the configuration. All integrals (B_0 and B_1 in subsonic or B in supersonic flow) are computed by numerical quadrature, using a scheme that is exact for $s=0$.

2.3. *Continuity at sonic flow*

The pressure kernel functions are shown in Table I. The steady kernel function can be obtained by putting $\bar{s}=0$ in the unsteady kernel function in Equation (3). If the parameters,

$$R_\pm = \mathrm{sqrt}[\xi^2+(\zeta_\pm)^2] \tag{12}$$

are defined, the right-hand side of the steady kernel function in subsonic flow can be integrated analytically.

$$B = \int_{-\infty}^{\zeta_-} \frac{\mathrm{d}v}{(v^2+\xi)^{3/2}} = \frac{1}{\xi^2}\left(\sqrt{\frac{\zeta_-}{\zeta_-^2+\xi^2}}+1\right) = \frac{1}{R_-(R_--\zeta_-)} \tag{13}$$

Then the steady kernel function in subsonic flow can be written as shown in Table II. The right-hand side of the steady kernel function in supersonic flow can be integrated analytically in the same manner as the kernel function in subsonic flow. It is difficult to tell whether they are continuous at sonic flow from the forms of the kernel function shown in Table II. Therefore, if the parameters

$$\zeta_\pm = (x \pm MR)/\beta \tag{14}$$

are defined, we can obtain the simpler form of the steady kernel functions as shown in Table III.

Table II. Steady non-planar kernel functions.

Kernel functions	K_{p0}
$M<1$	$\frac{1}{8\pi}\left[\frac{M}{RR_-}+\frac{1}{R_-(R_- - \zeta_-)}\right]$
$M>1$	$\frac{1}{8\pi}\left[\frac{M}{RR_-}+\frac{M}{RR_+}+\frac{1}{\xi^2}\left(\frac{\zeta_-}{R_-}-\frac{\zeta_+}{R_+}\right)\right]$

Table III. Continuity at sonic flow.

Kernel functions	$M<1$	$M=1$	$M>1$
K_{p0}	$\frac{R+X}{8\pi R\xi^2}$	$\frac{1}{4\pi\xi^2}$	$\frac{X}{4\pi R\xi^2}$

Considering the limit

$$\lim_{M\to 1} R = |X| \tag{15}$$

we can obtain the continuity of each kernel function listed in Table III.

3. RESULTS AND DISCUSSION

The lift curve slope, C_{L_α}, is one of the important characteristics of the wing. Normally, wings with large aspect ratio have relatively steep lift curves with clearly defined maximum values. In contrast, wings with a low aspect ratio show the opposite behaviour. Wings with a low aspect ratio therefore require higher angles of attack to produce a particular lift than wings with a high aspect ratio. The lift curve slopes become greater with increasing aspect ratio.

3.1. Steady results

In Figure 4, the convergence behaviour of lift curve slopes for a rectangular wing with aspect ratio of 5 at zero Mach number and 11.4° angle of attack is shown for the variation of span and chordwise panel numbers. An experimental result of Theil and Weissinger [19] is also plotted in the figure for comparison. The panels are constructed as quadrilaterals with side edges parallel to the flow. The control points are fixed along the midspan, at 85% local chord. This choice optimizes convergence rates with panel refinement. It can be seen in the figure that the agreement between the present method and experimental data is encouraging when 20 by 20 panel numbers is used for the prediction.

In Figure 5, to validate the present method for rectangular wings with various aspect ratios, results of the present analysis are compared with those of Ueda [15] which are based on DPM. Six chordwise and 16 spanwise panels are used for the present calculation whereas Ueda [15] used 20 chordwise square panels. As can be seen in the figure, the present results agree well with those of Ueda [15]. In the figure, the lift curve slope becomes greater with

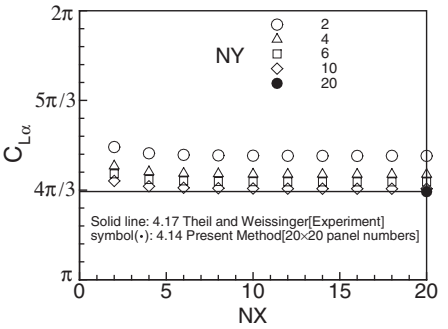

Figure 4. Lift curve slope convergence with respect to the number of panels for a rectangular wing with an aspect ratio of 5 at $M = 0$ and $\alpha = 11.4°$ (NX: chordwise panel numbers, NY: spanwise panel numbers).

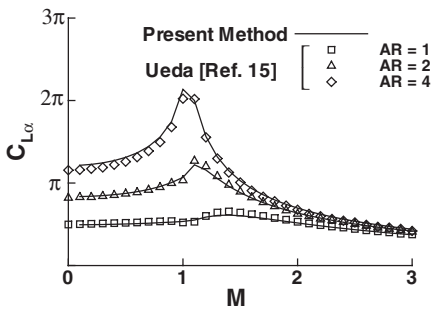

Figure 5. Lift curve slope of rectangular wings.

increasing Mach number in the range $M < 1$. At Mach numbers between 1.0 and 1.1 the lift curve slope reaches its highest value.

To clearly demonstrate the continuity of the numerical solutions near sonic conditions, further refined calculations have been carried out around sonic point. The detailed results in the transonic flow are shown in Figure 6. As seen in the figure, it can be concluded that the numerical values obtained by the present panel method are continuous at the sonic point.

The lift curve slope convergence for an untapered 45° swept wing at the sonic flow point is shown in Figure 7. The wing has the same aspect ratio of 5 as for the case in Figure 4. It can be easily seen from the figure that five chordwise and 10 spanwise panels are enough for the calculation of the lift curve slope of a swept wing as in the case of the rectangular wing in Figure 4.

Figure 8 compares the lift curve slopes vs Mach number for three swept wings calculated by the present method with the results of Ueda [15]. The wings have the same aspect ratio of 4 and a leading edge sweep back angle of 45° with different taper ratios. Ten chordwise and 28 spanwise panels are used for the present calculation. As can be seen in the figure, the present results are in good agreement with those of Ueda [15] as in the case of rectangular wings.

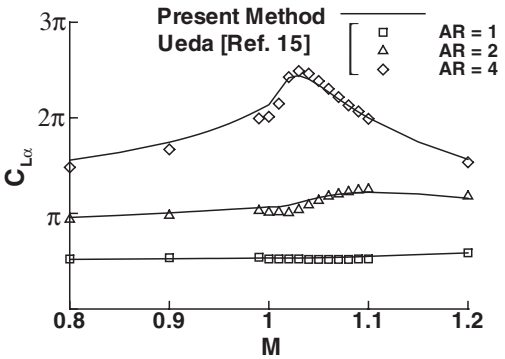

Figure 6. Detailed figure of Figure 5 at $M = 1$.

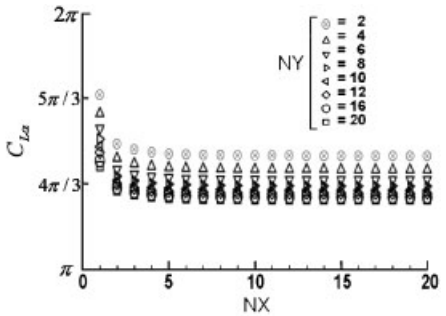

Figure 7. Lift curve slope convergence with respect to the number of panels for an untapered 45° swept wing at $M = 1$ (NX: chordwise panel numbers, NY: spanwise panel numbers).

Figure 9 compares the lift curve slopes vs Mach number for a supersonic transport wing by the present method to the results of Ueda [15]. The wing has an aspect ratio of 1.09 and a span of 0.98. The explicit specification of the wing can be found in Figure 9. The wing is discretized with five chordwise and 28 spanwise panels. It can be seen in the figure that the present results agree well with those of Ueda [15] and the numerical results are continuous at the sonic flow point.

3.2. Unsteady results

For the lack of three-dimensional unsteady results including the sonic flow point to compare, present results are validated by comparing the calculated results with those by the surface-loading method of Runyan and Woolston [16]. Runyan and Woolston [16] calculated the effect of Mach number on the aerodynamic characteristics of finite wings for a range of Mach numbers up to and including $M = 1$. They extended the subsonic kernel function method to the Mach one using the concepts of Falkner [20]. The results at supersonic speeds were obtained from Nelson *et al.* [21].

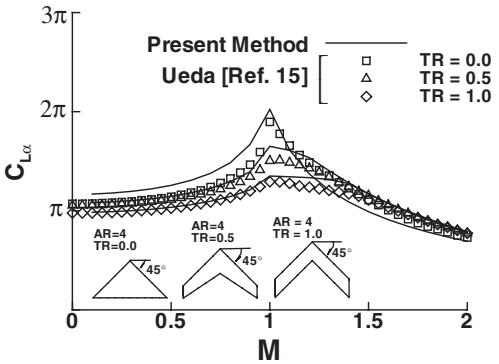

Figure 8. Lift curve slope vs Mach number for 45° swept wings with AR = 4.

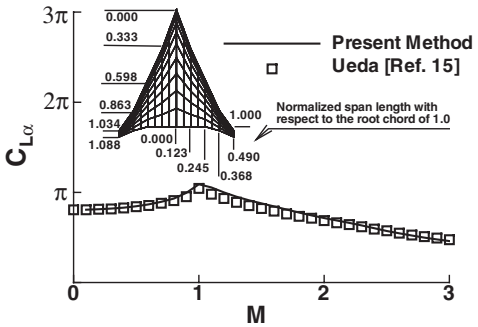

Figure 9. Lift curve slope of a supersonic transport wing.

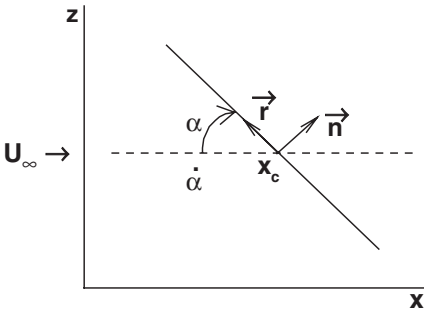

Figure 10. Co-ordinate system for the pitching motion.

Figure 10 shows the co-ordinate system for a wing in pitching motion at an angle of attack. The calculations have been carried out for a rectangular wing with aspect ratio of 2 and reduced frequency of 0.22 based on the semichord length. In the present calculation, the

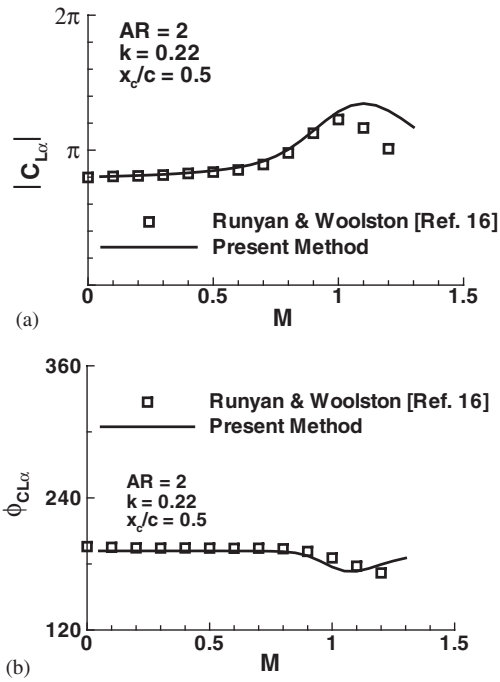

Figure 11. The unsteady lift curve slope of a rectangular wing oscillating in pitch about its mid-chord: (a) Magnitude, (b) phase angle.

wing is discretized with 30 chordwise and 20 spanwise panels. The point of evaluation of the unsteady factors has been set at the panel centroid. A better choice is the centroid of the generalized area, which would reduce the quadrature errors, especially for a panel containing singularities.

Figure 11 presents a comparison of the unsteady lift curve slope as calculated by the present method and that of Runyan and Woolston [16]. The magnitude of the lift curve slope, $|C_{L_\alpha}|$, and the corresponding phase angles of the lift curve slope, $\phi_{C_{L_\alpha}}$, with the change of Mach number are shown in the figure. It can be seen from the figure that the present result agrees well with that of Runyan and Woolston [16] except for the slight difference in the magnitude of the lift curve slope for the low supersonic flow speed.

One essential requirement for the flutter calculation is to predict the moment accurately [16]. Figure 12 presents a comparison of the pitching moment curve slope as calculated by the present method and that of Runyan and Woolston [16]. It can be seen from the two figures that the present result agrees well with that of Runyan and Woolston [16] except for the slight difference in the phase of the moment curve slope for the transonic speeds. The present results for unsteady motions are meaningful when the maneuver presents a certain degree of unsteadiness, and low-amplitude motion [22]. The present results show that present method can constitute a continuous bridging in the results from subsonic through transonic to supersonic speeds [23]. As shown in Figures 11 and 12, the compressibility effect on the lift and moment can be approximately predicted by use of the factor $\sqrt[4]{1-M^2}$ up to

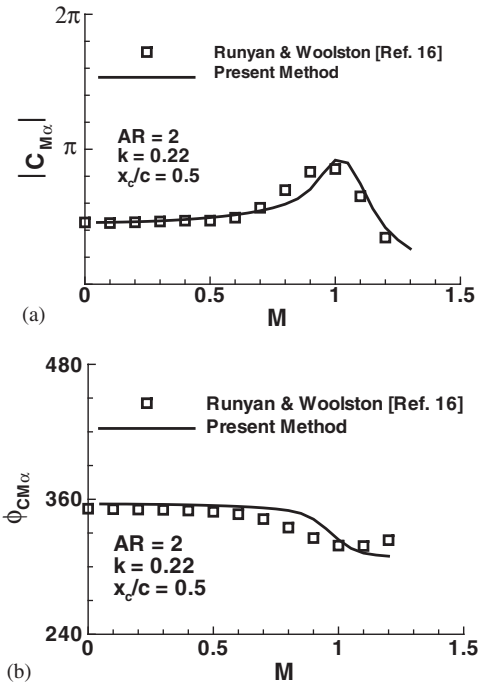

Figure 12. The unsteady moment curve slope of a rectangular wing oscillating in pitch about its mid-chord: (a) Magnitude, (b) phase angle.

$M = 0.7$ [16]. The magnitudes of the lift and moment increase around $M = 1$ and then decline at supersonic speed [16]. As discussed, the numerical results of Runyan and Woolston [16] agree well with the calculated results by the present method except for slight differences. This is remarkable, since the results of Runyan and Woolston [16] were obtained by hand evaluating few unknowns in the 1950s whereas the present method uses the modern computers.

4. CONCLUSION

The sonic kernel in steady or unsteady flow has been reduced to a simple form as a finite limit from both the subsonic and supersonic sides when the Mach number tends to one. For all speed ranges in the Laplace domain, the pressure kernel functions of the singular integral equation are defined, and their continuity at the sonic flow speed is verified.

The comparison of the present steady results with those of DPM shows the possible application of the present method to the airload calculations for all Mach numbers including the sonic point. For the lack of available unsteady results in the transonic flow speed to compare, the results for the pitching wing are compared to the other integral results. The good agreement validates the usefulness of the present method in evaluating unsteady aerodynamic performance parameters. The present method has the limitation on application to the thick

wing in the flow range near $M = 1$ where the flow non-linearity due to the thickness plays an important role.

ACKNOWLEDGEMENTS

This work was supported by grant No. (1999-1-305-001-5) from the Basic Research Program of the Korean Science and Engineering Foundation.

REFERENCES

1. Küssner HG. General lifting surface theory. *Allgemeine Tragflächentheorie*, *Luftfahrtforschung* 1940; **17**(11–12):370–378.
2. Küssner HG. General airfoil theory. *NACA TM*-979, 1941.
3. Landahl MT. Kernel function for nonplanar oscillating surfaces in a subsonic flow. *AIAA Journal* 1967; **5**(5):1045–1046.
4. Landahl MT, Stark V. Numerical lifting-surface theory-problems and progress. *AIAA Journal* 1968; **6**(11): 2049–2060.
5. Harder RL, Rodden WP. Kernel function for nonplanar oscillating surfaces in supersonic flow. *Journal of Aircraft* 1971; **8**(8):667–679.
6. Ueda T, Dowell EH. A new solution method for lifting surfaces in subsonic flow. *AIAA Journal* 1982; **20**(3):348–355.
7. Ueda T, Dowell EH. Doublet-point method for supersonic unsteady lifting surfaces. *AIAA Journal* 1984; **22**(2):179–186.
8. Ueda T. Lifting surface calculations in the Laplace domain with application to root loci. *AIAA Journal* 1987; **25**(5):698–704.
9. Tewari A. Doublet-point method for supersonic unsteady aerodynamics of nonplanar lifting-surfaces. *Journal of Aircraft* 1994; **31**(4):745–752.
10. Albano E, Rodden WP. A doublet-lattice method for calculating lift distributions on oscillating surfaces in subsonic flow. *AIAA Journal* 1969; **7**(2):279–284.
11. Kalman TP *et al*. Application of the doublet-lattice method to nonplanar configurations in subsonic flow. *Journal of Aircraft* 1971; **8**(6):406–413.
12. Eversmann W, Pitt DM. A hybrid doublet lattice-point method for general lifting surface configurations in subsonic flow. *AIAA Paper* 89-1322, 1989.
13. Cho J, Williams MH. S-plane aerodynamics of nonplanar lifting surfaces. *Journal of Aircraft* 1993; **30**(4): 433–438.
14. Cho J, Williams MH. Propeller-wing interaction using a frequency domain panel method. *Journal of Aircraft* 1990; **27**(3):196–203.
15. Ueda T. Continuity of lifting surface theory in subsonic and supersonic flow. *AIAA Journal* 1998; **36**(10): 1788–1791.
16. Runyan HL, Woolston DS. Method for calculating the aerodynamic loading on an oscillating finite wing in subsonic and sonic flow. *NACA Report* 1322, 1956.
17. Cho J. Frequency domain aerodynamic analysis of interacting rotating systems. *Ph.D. Dissertation*, Purdue University, 1978; 108–114.
18. Dowell EH, Curtis Jr HC, Scanlan RH, Sisto F. *A Modern Course in Aeroelasticity*. Sijthoff & Noordhoff International Publishers B.V.: Alphen aan den Rijn, The Netherlands, 1978; 159–266.
19. Theil A, Weissinger J. Pressure-distribution measurements on a straight and on a 35° swept-back tapered wing. *NACA TM* 1126, 1947.
20. Falkner VM. The calculation of aerodynamic loading on surfaces of any shape. *R. & M. No.* 1910, British A.R.C., August 1943.
21. Nelson HC, Rainey RA, Watkins CE. Lift and moment coefficients expanded to the seventh power of frequency for oscillating rectangular wings in supersonic flow and applied to a specific flutter problem. *NACA TN* 3076, 1954.
22. Bisplinghoff RL, Ashley H, Halfman, RL. *Aeroelasticity*. Addison-Wesley: Reading, MA, 1955; 375.
23. Garrick IE. Nonsteady wing characteristics. *High Speed Aerodynamics and Jet Propulsion*, vol. 7. Princeton University Press: Princeton, NJ, 1957; 678.

